

# Toward a Classification of Isodynamic Feed-Forward Motifs\*

Dewey T. Taylor<sup>1</sup>, John W. Cain<sup>1,3†</sup>, Danail G. Bonchev<sup>1,3</sup>, Stephen S. Fong<sup>2,3</sup>,  
Advait A. Apte<sup>2</sup>, and Lauren E. Pace<sup>1</sup>

<sup>1</sup>Department of Mathematics, 1015 Floyd Avenue, Virginia Commonwealth University  
Richmond, VA 23284 USA

<sup>2</sup>Department of Chemical and Life Science Engineering, 601 West Main Street, Room 403,  
P.O. Box 843028, Virginia Commonwealth University, Richmond, VA 23284-3028 USA

<sup>3</sup> Center for the Study of Biological Complexity, Trani Center for Life Sciences, P.O. Box 842030  
Virginia Commonwealth University, Richmond, VA 23284-2030 USA

July 28, 2009

## ABSTRACT

A preceding study analyzed how the topology of network motifs affects the overall rate of the underlying biochemical processes. Surprisingly, it was shown that topologically non-isomorphic motifs can still be *isodynamic* in the sense that they exhibit the exact same performance rate. Because of the high prevalence of feed-forward functional modules in biological networks, one may hypothesize that evolution tends to favor motifs with faster dynamics. As a step towards ranking the efficiency of feed-forward network motifs, we use a linear flow model to prove theorems establishing that certain classes of motifs are isodynamic. In partitioning the class of all motifs on  $n$  nodes into equivalence classes based upon their dynamics, we establish a basis for comparing the efficiency/performance rates of different motifs. The potential biological importance of the theorems is briefly discussed and is the subject of an ongoing large-scale project.

*Keywords:* feed-forward motif, isodynamic, ordinary differential equations

*AMS subject classifications:* 92C45, 34A30

## 1 Introduction

Biological research has been rapidly changing since the release of whole genome sequences. One of the central changes is a growing effort to study living systems as intact, integrated systems, thus giving rise to systems biology. Within the realm of systems biology, concurrent development of experimental and computational techniques has occurred. Experimental techniques primarily focus on quantitative measurements of system components whereas computational techniques provide an analytical framework for studying network properties and function. Studies on biological networks have resulted in many findings, including a general description of how biological networks are organized as scale-free networks [1, 2, 3] and specifically how different network motifs function [4, 5, 6, 7] within this framework.

---

\*This is a preprint of an article whose final and definitive form has been published in the Journal of Biological Dynamics, copyright 2009, Taylor & Francis. The Journal of Biological Dynamics is available online at <http://journalsonline.tandf.co.uk/>

†Corresponding author. E-mail: [jwcain@vcu.edu](mailto:jwcain@vcu.edu)

When studying biological networks in terms of functional subunits, it has been found that there are specific network motifs that are highly prevalent across different organisms. Specifically, feed-forward loops have been shown to be the single most commonly-occurring network motif [8, 9, 10, 11, 12] in biological systems. The structure of feed-forward loops can be found at all levels of biological systems including metabolic networks, transcriptional regulatory networks, and signaling networks. Feed-forward loops have also been studied within the context of different cellular processes [13, 14, 15, 16], due to the basic structure of propagating signals, and the overall dynamics of processes [17, 18, 19, 20, 21].

The identification and classification of biological network structures and motifs may play an important role in studying and understanding biology. The functionality of a biological system stems from both the attributes of individual components and also how these components are connected or interact with each other. The characterization of individual component functionality has a strong history in biological research whereas connectivity or interaction effects are largely still being determined. Thus, it is important to identify biological network motifs and also to have an analytical framework to characterize how the connectivity of a motif contributes to function.

This study stems from a previous work [22], in which cellular automata [22, 23, 24, 25, 26, 27] and ordinary differential equation modeling were applied to the search for network motif topologies that accelerate the overall biochemical process. The surprising finding that different network structures can lead to similar, isodynamic behavior [22], presented a mathematical framework for characterizing the dynamic behavior of feed-forward loops. In the present study, as a first step toward ranking the overall conversion speeds of various biochemical motifs, differential equation modeling is used to classify into equivalence classes different network topologies that demonstrate isodynamic behavior. Due to the prevalence of feed-forward motifs in biological systems, this work provides a mathematical basis for understanding many cellular processes and can be viewed as a demonstration of the need to develop mathematical interpretations of biological motifs.

## 2 Modeling the motif dynamics with ODEs

A network motif is a subgraph [28, 29] which is considerably more abundant in the network of interest than in the randomized network having the same size and vertex degree distribution. Given a feed-forward motif such as the one in Figure 1, corresponding to each vertex is a chemical species whose concentration we must track. In a slight abuse of notation, we shall identify each vertex label with the concentration of the species to which the vertex corresponds. We use systems of ordinary differential equations (ODEs) to model changes in concentrations. Instead of attempting a careful description of any nonlinear interactions between the various species, we assume that changes in concentrations are simply obtained by taking the difference between the flow into a vertex and the flow out of a vertex. In a previous study, we demonstrated that such linear models perform surprisingly well in predicting motif dynamics relative to standard nonlinear models (see Figure 6 in [22]). Among motifs classified as isodynamic by the linear model, the nonlinear model (Michaelis-Menten type) agrees that such motifs exhibit generally close performance times.

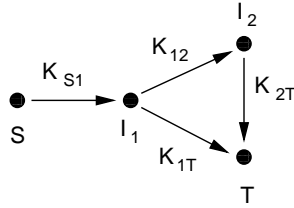


Figure 1: Example of a feed-forward motif with four vertices and four edges, explaining the notation used in the linear differential equations.

For example, the feed-forward motif in Figure 1 would give rise to a system of four ODEs

$$\begin{aligned} \frac{dS}{dt} &= -k_{S1}S, \\ \frac{dI_1}{dt} &= k_{S1}S - (k_{12} + k_{1T})I_1, \\ \frac{dI_2}{dt} &= k_{12}I_1 - k_{2T}I_2, \\ \frac{dT}{dt} &= k_{1T}I_1 + k_{2T}I_2, \end{aligned}$$

where  $k_{S1}$ ,  $k_{12}$ ,  $k_{1T}$ , and  $k_{2T}$  are rate constants associated with the four processes indicated by directed edges.

In matrix notation, this system can be written  $\mathbf{x}' = A\mathbf{x}$  where  $\mathbf{x}$  denotes the transpose of the vector  $[S, I_1, I_2, T]$  of unknowns, and

$$A = \begin{bmatrix} -k_{S1} & 0 & 0 & 0 \\ k_{S1} & -k_{12} - k_{1T} & 0 & 0 \\ 0 & k_{12} & -k_{2T} & 0 \\ 0 & k_{1T} & k_{2T} & 0 \end{bmatrix}$$

is the coefficient matrix. Observe that all columns sum to zero, a consequence of conservation of mass. Moreover, the rightmost column contains only zeros since the (T)arget vertex has outdegree zero.

The solution of the above linear, constant-coefficient system is given by  $\mathbf{x}(t) = e^{tA}\mathbf{x}(0)$ , where  $e^{tA}$  is the usual matrix exponential of  $A$  and  $\mathbf{x}(0)$  is a vector of initial concentrations of the four species involved in this reaction process.

**Isodynamic motifs.** Suppose that we wish to compare the dynamics of two non-isomorphic feed-forward motifs on  $n$  vertices,  $V_1, V_2, \dots, V_n$ . In order to establish a fair basis of comparison for the performance of the two motifs, we invoke the following assumptions. First, since our primary objective is to track each motifs' progress toward producing its target product(s), we must assume that the two motifs have the same number<sup>1</sup> of target vertices (sinks). Second, we must assume that both motifs start from the same initial conditions. Finally, we shall assume idealized reactions in which each process occurs at the same

<sup>1</sup>More exactly, we assume a one-to-one correspondence between the sets of target vertices for the two motifs, thereby allowing direct comparison of the accumulation of each target. This assumption is quite natural if, for example, we wish to compare the performance of the same biochemical network in two different organisms. Although network topology may differ from organism to organism, the network itself has the same biological functions (i.e., to produce the same targets).

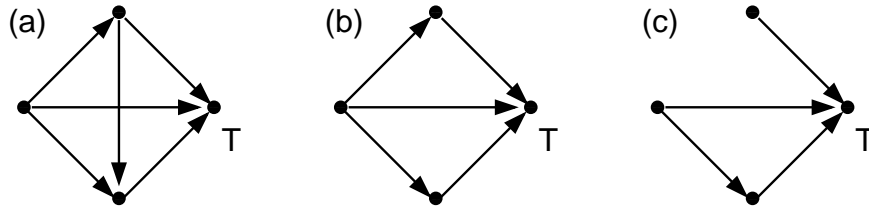


Figure 2: Examples of 4-vertex motifs with a single (T)target vertex of maximal indegree. Theorem 3.1 implies that these three motifs are isodynamic.

rate—i.e., all rate constants are equal and, without loss of generality, can be chosen to be 1. This assumption of uniform rate constants allows our analysis to focus on the specific effect of network topology on dynamic behavior.

Our primary emphasis is on motifs with precisely one source vertex and one target vertex, in which case we shall write  $S = V_1$  and  $T = V_n$ . Given a set of initial conditions, we can determine which motif is “faster” by solving two systems of ODEs and comparing the rates at which the (T)arget product is accumulated for each network. More exactly, suppose that  $A$  and  $B$  denote the coefficient matrices associated with the two systems of ODEs, and let  $\mathbf{x}_A(t)$  and  $\mathbf{x}_B(t)$  denote the solutions of the systems for the given set of initial conditions. The last entries in these vectors are  $T_A(t)$  and  $T_B(t)$ , formulas for the target product species for the two networks. Following [22], one may compare the speeds of the two networks by specifying some desired threshold level of conversion, say  $T_{thr}$ , and solving the equations  $T_A(t) = T_{thr}$  and  $T_B(t) = T_{thr}$  for  $t$ .

In what follows, we shall concern ourselves with networks which exhibit *exactly* the same performance, working under our above assumptions. We say that two networks with associated coefficient matrices  $A$  and  $B$  are *isodynamic* if  $T_A(t) = T_B(t)$  for all  $t$ , independent of the choice of initial conditions. The remainder of this paper is devoted to identifying classes of isodynamic networks.

### 3 Classes of isodynamic motifs

In this section, we identify two classes of isodynamic motifs and provide mathematical proof for the existence of isodynamicity. First, we consider those motifs whose target vertices have maximal indegree (see Figure 2). Then, we analyze a special class of networks known as biparallel motifs.

#### 3.1 Target vertices with maximal indegree

**Theorem 3.1.** *Consider the family of feed-forward motifs on  $n$  vertices with a single target vertex. Then all motifs for which the indegree of the target vertex is  $(n-1)$  are isodynamic.*

*Proof.* As in the previous Section, let  $V_1(t), V_2(t), \dots, V_n(t) = T(t)$  denote the concentrations of the  $n$  species involved in our biochemical reaction network. We remark that  $T(t)$  is the concentration of the target species and  $V_1(t)$  corresponds to a source<sup>2</sup> species. The system

<sup>2</sup>This proof allows for the possibility of multiple source nodes; see, for example, the motif in Figure 2c.

of ODEs governing the dynamics of the network can be written as  $\mathbf{x}'(t) = A\mathbf{x}(t)$ , where  $A$  is a coefficient matrix and  $\mathbf{x}$  is the vector

$$\mathbf{x}(t) = \begin{bmatrix} V_1(t) \\ V_2(t) \\ \vdots \\ V_{n-1}(t) \\ T(t) \end{bmatrix}. \quad (1)$$

Since the solution of this system is given by  $\mathbf{x}(t) = \exp(tA)\mathbf{x}(0)$ , it suffices to prove that the last row of the matrix  $\exp(tA)$  is the same for all motifs for which the indegree of the (T)target vertex is  $(n-1)$ . To do so, we make several observations about the structure of  $A$ :

*Observation 1:* Since the outdegree of the target vertex is zero, the last column of  $A$  consists only of zeros.

*Observation 2:* Since the indegree of the target vertex is  $(n-1)$ , all other vertices must have an edge directed toward the target vertex. Hence, the last row of  $A$  is  $[1, 1, 1, \dots, 1, 1, 0]$ .

*Observation 3:* Since we are dealing with a feed-forward motif, it is possible to order the vertices in such a way that there are no directed edges  $\overrightarrow{V_j V_k}$  if  $j > k$ . Hence, the  $(n-1) \times (n-1)$  matrix  $\mathbf{L}$  formed by excluding the last row and column of  $A$  will be lower triangular.

*Observation 4:* Since a directed edge  $\overrightarrow{V_j V_k}$  contributes 1 to the outdegree of  $V_j$  and 1 to the indegree of  $V_k$ , each column of  $A$  must sum to 0.

From the first three Observations, the matrix  $A$  has block structure

$$A = \left[ \begin{array}{c|c} & \begin{matrix} 0 \\ \vdots \\ 0 \end{matrix} \\ \hline \mathbf{L} & \\ \hline \begin{matrix} 1 & 1 & \dots & 1 \end{matrix} & \begin{matrix} 0 \\ 0 \end{matrix} \end{array} \right].$$

Squaring  $A$  yields

$$A^2 = \left[ \begin{array}{c|c} & \begin{matrix} 0 \\ \vdots \\ 0 \end{matrix} \\ \hline \mathbf{L}^2 & \\ \hline \begin{matrix} [1, 1, \dots, 1] \mathbf{L} \end{matrix} & \begin{matrix} 0 \\ 0 \end{matrix} \end{array} \right].$$

Note that the product  $[1, 1, \dots, 1]\mathbf{L}$  is a row vector whose entries are the sums of the columns of  $\mathbf{L}$ . By Observation 4, the columns of  $\mathbf{L}$  must sum to -1, which implies that

$$A^2 = \left[ \begin{array}{c|c} & \begin{matrix} 0 \\ \vdots \\ 0 \end{matrix} \\ \hline \mathbf{L}^2 & \\ \hline \begin{matrix} -1 & -1 & \dots & -1 \end{matrix} & \begin{matrix} 0 \\ 0 \end{matrix} \end{array} \right].$$

Straightforward induction shows that

$$A^m = \left[ \begin{array}{c|c} & \begin{matrix} 0 \\ \vdots \\ 0 \end{matrix} \\ \hline \mathbf{L}^m & \\ \hline \begin{matrix} (-1)^{m+1} & (-1)^{m+1} & \dots & (-1)^{m+1} \end{matrix} & \begin{matrix} 0 \\ 0 \end{matrix} \end{array} \right].$$

Finally, since

$$e^{tA} = \sum_{m=0}^{\infty} \frac{(tA)^m}{m!},$$

we find that the first  $(n - 1)$  entries of the last row are given by

$$\sum_{m=1}^{\infty} (-1)^{m+1} \frac{t^m}{m!} = - \sum_{m=1}^{\infty} \frac{(-t)^m}{m!} = 1 - \sum_{m=0}^{\infty} \frac{(-t)^m}{m!} = 1 - e^{-t},$$

and the last entry is simply 1. Thus, the last row of  $e^{tA}$  is

$$[1 - e^{-t}, 1 - e^{-t}, \dots, 1 - e^{-t}, 1]$$

independent of the precise form of  $\mathbf{L}$ . Taking the inner product of this vector with the vector of initial conditions yields a formula for  $T(t)$ .  $\square$

Theorem 3.1 is easily extended to motifs with multiple target vertices.

**Theorem 3.2.** *Suppose  $1 < k < n$  and consider the family of feed-forward motifs on  $n$  vertices with precisely  $k$  target vertices. Then all motifs for which the indegrees of the target vertices are  $(n-k)$  are pairwise isodynamic.*

*Proof.* Proceeding as in the proof of Theorem 3.1, the vertices can be ordered in such a way that (i) the last  $k$  entries in the vector of unknowns  $\mathbf{x}$  correspond to the target vertices, and (ii) the coefficient matrix takes the block form

$$A = \left[ \begin{array}{c|c} \mathbf{L} & 0 \\ \mathbf{M} & 0 \end{array} \right],$$

where  $\mathbf{L}$  is an  $(n - k) \times (n - k)$  lower-triangular matrix whose columns sum to  $-k$ , and  $\mathbf{M}$  is a  $k \times (n - k)$  matrix with a 1 in every entry. Exponentiating as before, one finds that

$$e^{tA} = \left[ \begin{array}{c|c} e^{t\mathbf{L}} & 0 \\ \frac{1 - e^{-kt}}{k} \mathbf{M} & \mathbf{I} \end{array} \right],$$

where  $\mathbf{I}$  denotes the  $k \times k$  identity matrix. Since the last  $k$  rows are independent of the form of  $\mathbf{L}$ , the theorem follows.  $\square$

### 3.2 Biparallel motifs

We now consider another special class of isodynamic motifs. Consider a motif formed by connecting the source vertex to the target vertex via two non-intersecting paths (see Figure 3). If the number of vertices is odd, the path lengths differ by one, and if the number of vertices is even, the two paths have equal length. We shall refer to these motifs as *biparallel* motifs.

In this section, we argue that adding certain edges, indicated by dashed lines in Figures 4a and 4b, to a biparallel motif on  $m$  vertices does not affect the dynamics. More exactly, if  $1 < k < (m - 1)$  and  $k$  has the same parity as  $m$ , then adding an edge between vertices  $k$  and  $k + 1$  has no effect on the dynamics, independent of the orientation of the edge.











and the sizes of the blocks are as indicated in the array

$$\left[ \begin{array}{c|c|c} (k-1) \times (k-1) & (k-1) \times 2 & (k-1) \times (m-k-1) \\ \hline 2 \times (k-1) & 2 \times 2 & 2 \times (m-k-1) \\ \hline (m-k-1) \times (k-1) & (m-k-1) \times 2 & (m-k-1) \times (m-k-1) \end{array} \right]. \quad (8)$$

The  $n$ th power of  $A + B$  has the block lower-triangular form

$$(A + B)^n = \left[ \begin{array}{c|c|c} [A_{11}]^n & & \\ \hline C_{21} & [A_{22} + B_{22}]^n & \\ \hline C_{31} & C_{32} & [A_{33}]^n \end{array} \right]. \quad (9)$$

The precise form of the blocks below the main diagonal is not important, we need only use the fact that, by inductive hypothesis, the last row of the matrix in (9) is identical to the last row of  $A^n$ . We now multiply (9) by  $(A + B)$  to obtain

$$\begin{aligned} (A+B)^{n+1} &= \left[ \begin{array}{c|c|c} [A_{11}]^n & & \\ \hline C_{21} & [A_{22} + B_{22}]^n & \\ \hline C_{31} & C_{32} & [A_{33}]^n \end{array} \right] \left[ \begin{array}{c|c|c} A_{11} & & \\ \hline A_{21} & A_{22} + B_{22} & \\ \hline A_{31} & A_{32} & A_{33} \end{array} \right] \\ &= \left[ \begin{array}{c|c|c} [A_{11}]^{n+1} & & \\ \hline C_{21}A_{11} + [A_{22} + B_{22}]^n A_{21} & [A_{22} + B_{22}]^{n+1} & \\ \hline C_{31}A_{11} + C_{32}A_{21} + [A_{33}]^n A_{31} & C_{32}[A_{22} + B_{22}] + [A_{33}]^n A_{32} & [A_{33}]^{n+1} \end{array} \right] \quad (10) \end{aligned}$$

To complete the proof, we must establish that the last row of matrix (10) is identical to the last row of  $A^{n+1}$ . Focus on the three lower blocks in (10) separately:

- Consider the last block in the last row of (10). Clearly,  $[A_{33}]^{n+1}$  is identical to the corresponding block in the matrix  $A^{n+1}$ , and therefore the last rows of  $(A + B)^{n+1}$  and  $A^{n+1}$  are the same in the last  $(m - k - 1)$  columns.
- Consider the first block in the last row of (10). The last row of this block is

$$[\text{last row of } C_{31}]A_{11} + [\text{last row of } C_{32}]A_{21} + [A_{33}]^n A_{31}. \quad (11)$$

By our inductive assumption, the last rows of  $C_{31}$  and  $C_{32}$  are the same as the last rows in the corresponding blocks of  $A^n$ . It follows immediately that the entries in (11) are identical to the entries in the the first  $(k - 1)$  columns of the last row of  $A^{n+1}$ .

- Finally, consider the middle block in the last row of (10). If we can argue that the last row of the matrix  $C_{32}B_{22}$  contains all zeros, then an argument similar to the one in the previous case shows that the last rows of  $A^{n+1}$  and  $(A + B)^{n+1}$  agree in columns  $k$  and  $k + 1$ , completing our proof. By inductive assumption, the last row of  $C_{32}$  is identical to the last row of the corresponding block in  $A^n$ . By Lemmas 3.4– 3.3, the entries in the last row of  $A^n$  come in *pairs*. Due to the form of the matrix  $B_{22}$ , the last row of  $C_{32}B_{22}$  is given by

$$[A_{m,k+1}^n - A_{m,k}^n, 0].$$

If the parity of  $m$  and  $k$  are the same and  $1 < k < (m - 1)$ , then Lemmas 3.4– 3.3 guarantee that the  $(m, k + 1)$  and  $(m, k)$  entries of  $A^n$  are identical. Therefore, with these restrictions on  $k$ , we find that the last row of  $C_{32}B_{22}$  is all zero. It follows that

the last rows of  $A^{n+1}$  and  $(A + B)^{n+1}$  agree in columns  $k$  and  $k + 1$ , and the proof is complete.

The exact same argument works if we reverse the orientation of the added edge, from vertex  $(k + 1)$  to vertex  $k$ . The only change is that the matrix  $B_{22}$  in (7) is replaced with

$$B_{22} = \begin{bmatrix} 0 & 1 \\ 0 & -1 \end{bmatrix}.$$

□

Lemma 3.5 is easily extended to the case in which we add multiple edges of the type indicated by dashed edges in Figure 4.

**Lemma 3.6.** *Suppose  $B$  is the matrix associated with adding several directed edges of the type described in Lemma 3.5. Then the last row of  $A^n$  is identical to the last row of  $(A + B)^n$  for all non-negative integers  $n$ .*

*Proof.* Use the same inductive argument as in the proof of Lemma 3.5. We remark that the sizes of the blocks in (8) will change and, in particular, the square block  $B_{22}$  will be larger than  $2 \times 2$ . By hypothesis,  $B_{22}$  will have an even number of rows and columns and can be subdivided into  $2 \times 2$  blocks, each of which has one of the following forms:

$$\begin{bmatrix} 0 & 0 \\ 0 & 0 \end{bmatrix}, \quad \begin{bmatrix} -1 & 0 \\ 1 & 0 \end{bmatrix}, \quad \begin{bmatrix} 0 & 1 \\ 0 & -1 \end{bmatrix}.$$

Moreover, the rows of  $B_{22}$  contain at most one non-zero entry and the columns of  $B_{22}$  contain at most two non-zero entries. Consequently, the same fortuitous cancellations that carried the proof of Lemma 3.5 will extend to this more general case. □

We now state our main result, which identifies a particular class of isodynamic motifs.

**Theorem 3.7.** *Consider the biparallel motif on  $m$  vertices, with the alternating vertex labeling given in Figure 3. Suppose we construct a new motif by adding directed edges as described in the hypotheses of Lemma 3.6. That is, we allow an edge to be added between vertices  $k$  and  $(k + 1)$  (regardless of orientation) if  $k$  has the same parity as  $m$  and  $1 < k < (m - 1)$ . Then this new motif is isodynamic with the biparallel motif.*

*Proof.* Let  $A$  denote the matrix (2) associated with the biparallel motif on  $m$  vertices, and let  $B$  denote the matrix associated with the added edge(s). By Lemma 3.6, the last row of  $A^n$  is identical to the last row of  $(A + B)^n$ . It follows that the matrices  $e^{tA}$  and  $e^{t(A+B)}$  have the same last row. Now consider the two systems of ODEs

$$\mathbf{x}'(t) = A\mathbf{x}(t) \quad \text{and} \quad \mathbf{x}'(t) = (A + B)\mathbf{x}(t), \quad (12)$$

where  $\mathbf{x}$  is the vector of unknowns in (1). The solutions of these two systems are

$$\mathbf{x}(t) = e^{tA}\mathbf{x}(0) \quad \text{and} \quad \mathbf{x}(t) = e^{t(A+B)}\mathbf{x}(0), \quad (13)$$

respectively. Since  $e^{tA}$  and  $e^{t(A+B)}$  have the same last row, the formulas for  $T(t)$  are identical regardless of the initial conditions  $\mathbf{x}(0)$ . Hence, adding edges of the type indicated by dashed lines in Figure 4 will always yields a motif that is isodynamic with the biparallel motif. □

## 4 Discussion and conclusions

In this paper, we have identified two classes of isodynamic feed-forward networks: those whose target vertices have maximal indegree, and biparallel networks with appropriately added edges (Figure 4). The feed-forward motifs studied here are comparable to the coherent type-1 motif that is the most prevalent type of feed-forward motif found in biological systems [30]. We model the dynamics of conversion of a source substrate into a target one using linear systems of ODEs, tracking changes in concentration by measuring “flow in minus flow out”. To study the effects of network topology, we considered the idealized case in which all reaction processes proceed at the same rate. Despite these assumptions, we are encouraged that numerical simulations with more realistic nonlinear ODE models suggest that even the linear model can be quite successful in identifying isodynamic networks [22].

In moving towards studying biology as intact systems, there is a growing need to characterize functional motifs (biological subsystems) that are commonly found in all organisms. The results of this study demonstrate the utility of applying mathematical analysis to describe dynamic behavior of feed-forward loops leading specifically to mathematical proof of the existence of isodynamic network topologies. In biological terms, this finding shows that there are multiple equivalent ways for the components of biological systems to be connected that would result in identical functional behavior in terms of the dynamics of converting one input to a desired output. This applies to all levels of biological networks including metabolic, regulatory, and signaling networks. Mathematical analysis of network motifs provides a rigorous framework for identifying general functional principles found in biological systems. The natural ensuing questions are if and why do biological systems favour the implementation of certain motifs when more than one option may provide similar functional outputs.

By partitioning the class of all feed-forward networks on  $n$  vertices into isodynamic equivalence classes, we establish a basis of performance comparison for different networks. There are compelling reasons to rank non-isodynamic networks according to speed, measuring the time required for each network to accumulate a specified amount of the target product starting from the same set of initial conditions. Indeed, among the feed-forward networks that appear in signaling pathways, it is of great interest to determine whether faster networks are favored by evolution. A subsequent study [31] investigates the abundance of motifs in metabolic networks and their compacted version called networks of interacting pathways (NIP). A node in a NIP represents a metabolic pathway, whereas a link stands for two pathways sharing a common metabolite. The preliminary results indicate a systemic prevalence of the 4-node feed-forward motif (a), shown in Figure 5 to all other NIP 4-node motifs having one source and one target node. For example, the most highly connected motif (a) in the network of interacting metabolic pathways of the bacteria *Staphylococcus aureus* subsp. *aureus* COL was prevalent in abundance (6.46%), followed by motif (b) (2.85%). Using systems of linear ODEs to model the dynamics of these networks, it is straightforward to show that the topology of motif (5a) is considerably faster than that of (5b) in conversion of the source substrate S into the target product T. The high abundance of this motif evidences that evolution conserves this effective topology of maximum cross-talk between the individual metabolic pathways. Another very interesting conclusion may be drawn from the lack of statistically significant abundance of the triparallel subgraph (5c), which can be obtained from the leading motif (5a) by deleting the directed edge between the two intermediate

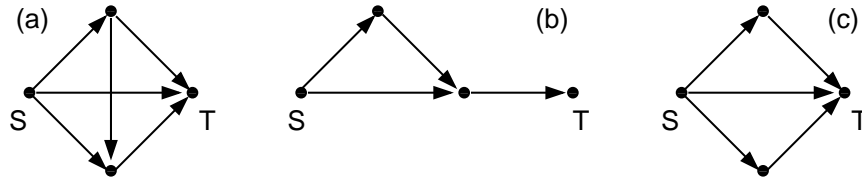


Figure 5: Examples of different 4-vertex motifs that occur with much different abundances in the metabolic network of the bacteria SAC. Motif (a) is faster and more prevalent than motifs (b) and (c).

nodes. According to Theorem 3.1, these two motifs are isodynamic—i.e., they would be equally effective with respect to the  $S \rightarrow T$  conversion. One might wonder why these motifs are not equally abundant. The most logical explanation would be that (at equal efficacy) evolution selects and conserves the structure that provides a higher stability (resilience to attack). Having an extra edge which does not contribute to a higher conversion rate is a beneficial redundancy; if this edge is destroyed or incapacitated, the efficacy of performance of the biochemical reactions will remain intact. Similar arguments are indeed valid for the biological relevance of Theorem 3.7: adding additional forward directed edges to the basic biparallel structure does not change dynamics and performance, but it increases network stability by introducing a beneficial redundancy. A large-scale study is in progress [31] to verify and generalize these preliminary conclusions.

### Acknowledgments

The sixth author gratefully acknowledges the financial support of the VCU Honors Summer Undergraduate Research Program.

### References

- [1] A.L. Barabási and R. Albert, *Emergence of scaling in random networks*, Science 286 (1999), pp. 509–512.
- [2] H. Jeong, B. Tombor, R. Albert, Z.N. Oltvai, and A.L. Barabási, *The large-scale organization of metabolic networks*, Nature 407 (2000), pp. 651–654.
- [3] M. Arita, *Scale-freeness and biological networks*, J. Biochem. 138 (2005), pp. 1–4.
- [4] R. Milo, S. Shen-Orr, S. Itzkovitz, N. Kashtan, D. Chklovskii, and U. Alon, *Network motifs: Simple building blocks of complex networks*, Science 298 (2002), pp. 824–827.
- [5] N. Kashtan, S. Itzkovitz, R. Milo, and U. Alon, *Topological generalizations of network motifs*, Phys. Rev. E 70 (2004), pp. 031909.
- [6] U. Alon, *An Introduction to Systems Biology: Design Principles of Biological Circuits*, CRC Press, Boca Raton, FL, 2006.
- [7] U. Alon, *Network motifs: Theory and experimental approaches*, Nature Rev. Genet. 8 (2007), pp. 450–461.

- [8] S.L. Wong, L.V. Zhang, A. Tong, Z. Li, D.S. Goldberg, O.D. King, G. Lesage, M. Vidal, B. Andrews, H. Bussey, C. Boone, and F.P. Roth, *Combining biological networks to predict genetic interactions*, Proc. Natl. Acad. Sci. USA 101 (2004), pp. 15682–15687.
- [9] J.S. Mattick, *A new paradigm for developmental biology*, J. Experimental Biol. 210 (2007), pp. 1526–1547.
- [10] R. Milo, S. Itzkovitz, N. Kashtan, R. Levitt, S. Shen-Orr, I. Ayzenshtat, M. Sheffer, and U. Alon, *Superfamilies of evolved and designed networks*, Science 303 (2004), pp. 1538–1542.
- [11] N. Kashtan and U. Alon, *Spontaneous evolution of modularity and network motifs*, Proc. Natl. Acad. Sci. USA 102 (2005), pp. 13773–13778.
- [12] S. Mangan and U. Alon, *Structure and function of the feed-forward loop network motif*, Proc. Natl. Acad. Sci. USA 100 (2003), pp. 11980–11985.
- [13] R. Dobrin, Q.K. Beg, A.L. Barabási, and Z.N. Oltvai, *Aggregation of topological motifs in the E. coli transcriptional regulatory network*, BMC Bioinformatics 5 (2004), pp. 10.
- [14] T. Palomero, W.K. Lim, D.T. Odom, M.L. Sulis, P.J. Real, A. Margolin, K.C. Barnes, J. O’Neil, D. Neuberg, A.P. Weng, J.C. Aster, F. Sigaux, J. Soulier, A.T. Look, R.A. Young, A. Califano, and A.A. Ferrando, *NOTCH1 directly regulates c-MYC and activates a feed-forward-loop transcriptional network promoting leukemic cell growth*, Proc. Natl. Acad. Sci. USA 103 (2006), pp. 18261–18266. See also “Correction” in Proc. Natl. Acad. Sci. USA 104 (2007), pp. 4240.
- [15] V.A. Klyachko and C.F. Stevens, *Excitatory and feed-forward inhibitory hippocampal synapses work synergistically as an adaptive filter of natural spike trains*, PLoS Biol. 4 (2006), pp. e207.
- [16] O.X. Cordero and P. Hogeweg, *Feed-forward loop circuits as a side effect of genome evolution*, Mol. Biol. Evol. 23 (2006), pp. 1931–1936.
- [17] Y. Qi and H. Ge, *Modularity and dynamics of cellular networks*, PLoS Comp. Biol. 2 (2006), pp. e174.
- [18] R.J. Prill, P.A. Iglesias, and A. Levchenko, *Dynamic properties of network motifs contribute to biological network organization*, PLoS Biol. 3 (2005), pp. e343.
- [19] V.P. Zhigulin, *Dynamical motifs: Building blocks of complex dynamics in sparsely connected random networks*, Phys. Rev. Lett. 92 (2004), pp. 238701.
- [20] J. Sardanyés and R.V. Solé, *Spatio-temporal dynamics in simple asymmetric hypercycles under weak parasitic coupling*, Physica D 23 (2007), pp. 116–129.
- [21] J.-D.J. Han, N. Bertin, T. Hao, D.S. Goldberg, G.F. Berriz, L.V. Zhang, D. Dupuy, A.J.M. Walhout, M.E. Cusick, F.P. Roth, and M. Vidal, *Evidence for dynamically organized modularity in the yeast protein-protein interaction network*, Nature 430 (2004), pp. 88–93.

- [22] A.A. Apte, J.W. Cain, D.G. Bonchev, and S.S. Fong, *Cellular automata simulation of topological effects on the dynamics of feed-forward motifs*, J. Biol. Eng. 2:2 (2008), pp. 1–12.
- [23] S. Wolfram, *A New Kind of Science*, Wolfram Media, Inc. Champaign, IL, 2002.
- [24] A. Deutsch and S. Dormann, *Cellular Automaton Modeling of Biological Pattern Formation*, Birkhäuser, Boston, MA, 2005.
- [25] L.B. Kier, C.-K. Cheng, B. Testa, and P.-A. Carrupt, *A cellular automata model of enzyme kinetics*, J. Molec. Graphics 14 (1996), pp. 227–231.
- [26] L.B. Kier, D.G. Bonchev, and G.A. Buck, *Modeling biochemical networks: A cellular automata approach*, Chem. Biodiversity 2 (2005), pp. 233-243.
- [27] D.G. Bonchev, L.B. Kier, and C.-K. Cheng, *Cellular automata (CA) as a basic method for studying network dynamics*, Lecture Series on Computer and Computational Sciences, VSP International Science Publishers, Leiden, Netherlands, Vol. 6 (2006), pp. 581–591.
- [28] F. Harary, *Graph Theory*, Addison-Wesley, Reading, MA, 1969.
- [29] *Handbook of Graph Theory*, J.L. Gross and J. Yellen, eds., CRC Press, Boca Raton, FL, 2004.
- [30] S. Mangan, S. Itzkovitz, A. Zaslaver, and U. Alon, *The incoherent feed-forward loop accelerates the response-time of the gal system of Escherichia coli*, J. Mol. Biol. 356 (2006), pp. 1073–1081.
- [31] D.G. Bonchev, M.R. Woodcock, A. Mazurie, D.T. Taylor, J.W. Cain, A.A. Apte, and S.S. Fong, work in progress, 2009.